Matter

CellPress

Review

Reviving the lithium-manganese-based layered oxide cathodes for lithium-ion batteries

Shiqi Liu,[1,2,2] Boya Wang,[1,2,2] Xu Zhang,[1,2] Shu Zhao,[1,2] Zihe Zhang,[1,2] and Haijun Yu[1,2,3,*]

SUMMARY

In the past several decades, the research communities have witnessed the explosive development of lithium-ion batteries, largely based on the diverse landmark cathode materials, among which the application of manganese has been intensively considered due to the economic rationale and impressive properties. Lithium-manganese-based layered oxides (LMLOs) are one of the most promising cathode material families based on an overall theoretical evaluation covering the energy density, cost, eco-friendship, etc. Unfortunately, the Mn^{3+} cation introduces severe Jahn–Teller (J–T) effect, which profoundly distorts the localized lattice structure and reduces the electrochemical stability. This perspective presents the principal comprehensions of the J–T effect in LMLOs and offers an outline picture of material design to suppress it. We outline the history of material design and further assess available approaches to address the J–T effect. Finally, we tentatively propose promising design trends with eliminated J–T effect to revive this important cathode material family toward practical applications.

INTRODUCTION

Lithium-ion batteries (LIBs) are the pivotal electrical power component of electric vehicles (EVs) and electronic devices, and evolve ubiquitously in human daily life.[1–5] The 2019 Nobel Prize in Chemistry awarded to John B. Goodenough, M. Stanley Whittingham, and Akira Yoshino further promotes the interests and research highlights of rechargeable batteries in modern society. The well-developed layered $LiCoO_2$ has occupied large market share for cathode since Sony Corporation coupled it with a graphite anode to realize commercial LIBs in 1991. Due to the shortcomings of $LiCoO_2$, such as the inadequate energy density, expensive ingredients, environmental pollution and unsustainability, and nickel-rich low-/zero-cobalt layered cathode materials ($LiNi_{0.8}Co_{0.15}Al_{0.05}O_2$, $LiNi_{0.9}Mn_{0.1}O_2$, $LiNiO_2$, etc.) have emerged as promising alternatives to $LiCoO_2$ for meeting the high demands of EVs.[6–8] However, these Ni-rich materials still suffer from drawbacks, such as unstable structures, undesirable phase transformations, limited thermal/cyclic stability, and insufficiently reduced cost.[9] Considering the growing application requests and concerns about economics and toxicity, cathode materials (layered oxides, spinels, etc.) with manganese as the dominant transition metal (TM) element have seen renewed interest, and show great potential for mass production capability of high-energy-density LIBs.

Among various Mn-dominant (Mn has the highest number of atoms among all TM elements in the chemical formula) cathode materials, lithium-manganese-based oxides (LMO), particularly lithium-manganese-based layered oxides (LMLOs), had been investigated as potential cathode materials for a long period. Unfortunately, many

Progress and potential

The layered oxide cathode materials for lithium-ion batteries (LIBs) are essential to realize their high energy density and competitive position in the energy storage market. However, further advancements of current cathode materials are always suffering from the burdened cost and sustainability due to the use of cobalt or nickel elements. Lithium-manganese-based layered oxides (LMLOs) hold the prospect in future because of the superb energy density, low cost, etc. Nevertheless, the key bottleneck of the development of LMLOs is the Jahn–Teller (J–T) effect caused by the high-spin Mn^{3+} cations. In general, J–T distortion of MnO_6 octahedra in LMLOs can result in the violent structural instability and further degradation during electrochemical cycling, which is fatal for its practical applications. Once the J–T effect is well eliminated by advanced material design strategies, the revival of LMLOs as commercial LIB cathode materials is highly anticipated.

drawbacks, such as the poor cyclic stability, voltage decay, difficulties in forming layered phases, and structural degradation, were not overcome at the early stages and thus greatly hindered the practical applications of LMLOs.[10,11] Significantly, a key issue in these materials is the Jahn–Teller (J–T) effect, which describes that any non-linear molecular system with a spatially degenerate electronic ground state undergoes a geometrical distortion to lower the overall energy and remove this degeneracy, resulting in the difficulty in formation of LMLOs and structural deterioration during electrochemical processes. Due to the existence of the high-spin Mn^{3+} in the octahedral MnO_6 units of LMLOs, the J–T effect is severe, which has significant adverse effects on the structural stability and electrochemical performances. Although hindered by the diverse drawbacks, particularly those induced by the J–T effect, LMLOs still have great advantages and potentials in the battery field since these drawbacks are expected to be solved with the fast development of material science and related techniques. Recently, many effective strategies have been proposed to eliminate the J–T effect for enhanced electrochemical performance of LMLOs, such as element substitution/doping of Mn and microstructural design.[12–19] Once the adverse effects that originate because of the J–T effect are well solved, the overall performance of LMLOs is expected to be greatly improved, which could signal a revival soon.

Here, we present a personal perspective on the status and further development of LMO cathodes based on the analysis of the development history and recent progress. In particular, among various LMO cathodes, LMLOs possess many advantages, including high energy density, desirable capacity, and low cost, which show great promise for the next-generation high-energy-density LIBs. However, the current exploration of LMLOs is far from enough because of the J–T effect in the Mn–O frameworks. Therefore, this perspective emphasizes the understanding of the J–T effect, particularly in LMLOs for LIBs, and strategies to eliminate the undesired J–T distortion. Although progress on LMLOs has been gradually implemented, it is not sufficient to meet the practical demands. It is thus critical and timely to summarize, discuss, and estimate LMLOs from the viewpoint of the J–T effect. We must push back the frontiers of the J–T effect in the years to come.

Elemental manganese for LIBs

From an industrial point of view, the quests for prospective LIBs significantly lie in the areas of energy density, lifespan, cost, and safety. Lithium-TM-based oxides are the most mature cathode materials for LIBs, and the adoption of TMs is of the primary importance. Although various TMs have been used to design cathode materials, Mn, Ni, and Co are the most commonly used elements in commercial cathode materials. In particular, among the three TMs, Mn possesses notable advantages in several aspects. First, Mn has a much higher crust abundance (950 ppm) than Ni (84 ppm) and Co (25 ppm), and thus its products have higher annual mine production and lower cost (Figure 1A).[42] According to the latest 5-year mineral commodity summaries, the price of Mn metallurgical ore is only ~0.7 USD/kg, less than 7% and 1.4% of Ni (>10 USD/kg) and Co (>50 USD/kg) metallurgical ore prices, respectively.[43] Second, owing to its specific atomic/electronic structure, Mn yields the derivative Li_2MnO_3 as a crucial component for the design of O anionic redox-activated cathode materials, particularly Li-rich layered oxides (LLOs), which can deliver much higher capacities and energy densities than traditional cathode materials. Third, Mn has a lower atomic weight (54.94) than Ni (58.69) and Co (58.93), which is beneficial for increasing the capacity of cathode materials. For example, the theoretical specific capacity of $LiMnO_2$ (285 mAh g^{-1}) is higher than those of $LiCoO_2$ (274 mAh g^{-1}) and $LiNiO_2$ (275 mAh g^{-1}). Fourth, owing to its lower toxicity than those of Ni and Co, Mn causes less-severe heavy metal pollution of the environment.[42] Considering

[1]Institute of Advanced Battery Materials and Devices, Faculty of Materials and Manufacturing, Beijing University of Technology, Beijing, 100124, P. R. China

[2]Key Laboratory of Advanced Functional Materials, Ministry of Education, Beijing University of Technology, Beijing, 100124, P. R. China

[2]These authors contributed equally

[3]Lead contact

*Correspondence: hj-yu@bjut.edu.cn

https://doi.org/10.1016/j.matt.2021.02.023

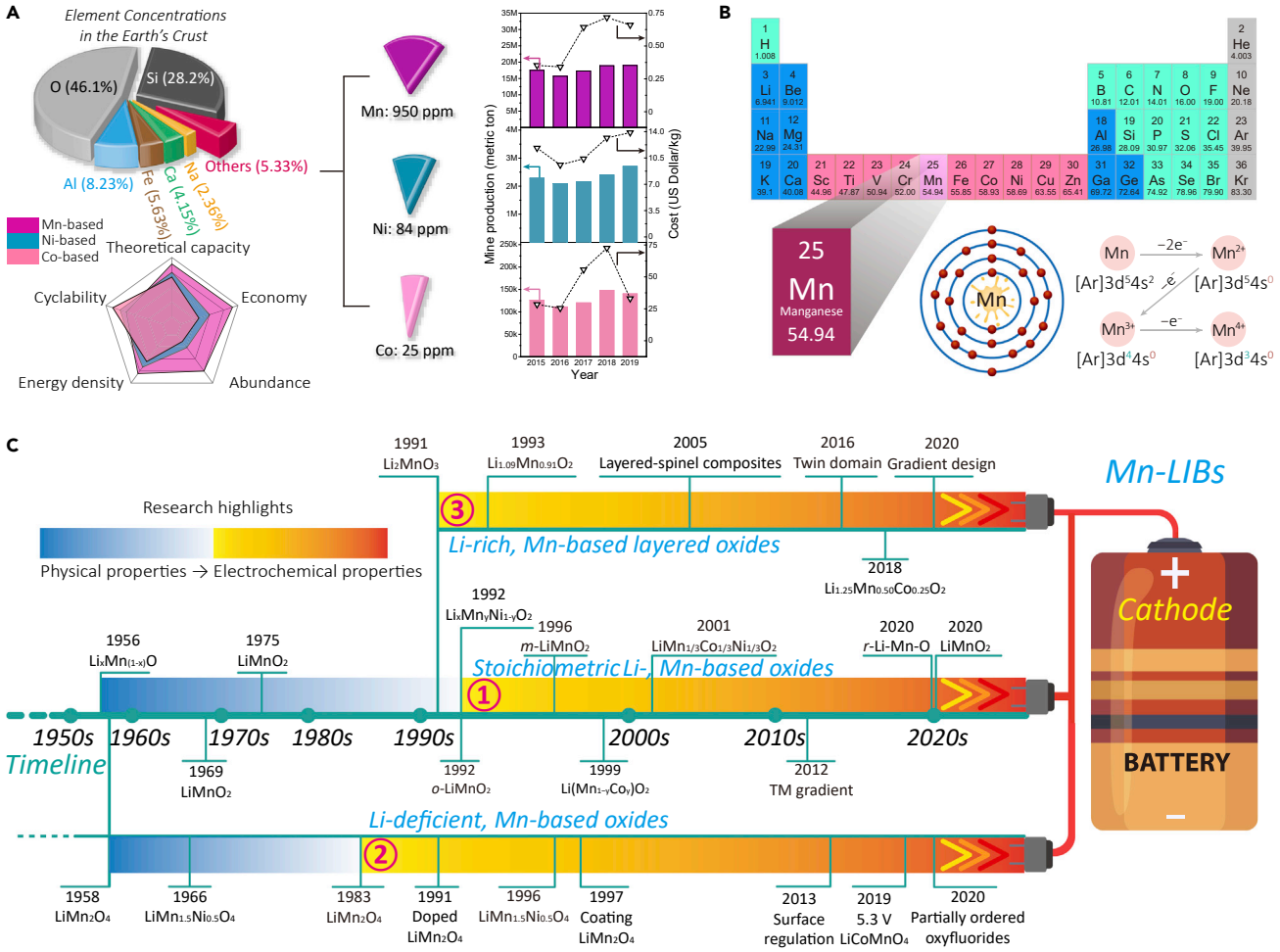

Figure 1. An outline of Mn used in cathode materials for LIBs

(A) Advantages of Mn compared with Ni and Co, in terms of crust abundance, characteristics of $LiTMO_2$ (TM = Mn, Ni, Co), and annual mine productions and costs.

(B) The atomic structure of Mn and its typical valence states in cathode materials.

(C) The development timelines of typical LMOs, including (1) stoichiometric $LiTMO_2$-type (Li/TM = 1), (2) Li-deficient (Li/TM < 1), and (3) Li-rich (Li/TM > 1) Mn-based oxides.[10,11,18–41]

these advantages, the re-examination, optimization, and new design of LMLOs, with the intention to increase the fraction of Mn among TMs, are essential for the development of better cathode materials.

As one of the 3*d* TMs, Mn exhibits a variety of oxidation states up to +7, among which the electrochemical activity usually occurs between +2 and +4 valences. The electron configurations of $Mn^0/Mn^{2+}/Mn^{3+}/Mn^{4+}$ are displayed in Figure 1B. In particular, when octahedrally coordinated with O, such as in $LiMnO_2$, Mn^{3+} with the $3d^4$ configuration usually presents with an asymmetric electron occupation in Mn e_g orbitals and a high-spin state. In this case, the J–T effect can easily occur, resulting in violent distortions of the Mn–O octahedra and instability of crystal lattices. On the other hand, the J–T effect is absent in Mn^{2+} and Mn^{4+} ions due to the different electron configurations, which is beneficial for the stability of the derived materials. Therefore, to improve the electrochemical stability of LMOs, one of the central concerns is the elimination of the Mn^{3+} high-spin state and the resulting J–T effect throughout the dynamic electrochemical process.

The studies of LMOs as LIB cathode materials can be dated back to the mid-20th century. Besides the layered structures of LMOs, the crystal structures show diverse types, such as spinel, rocksalt structure, etc. At the early research stage of LMOs, the two named crystal structures are more easily fabricated because of the intrinsic interactions of Mn^{3+} cations, which should not be neglected in the development of LMLOs.[44] According to the Li/Mn stoichiometric ratio, which profoundly determines their crystal structures and electrochemical behaviors, LMOs can be categorized into three types, including (1) stoichiometric $LiTMO_2$-type (Li/TM = 1), (2) Li-deficient (Li/TM < 1), and (3) Li-rich (Li/TM > 1) materials (Figure 1C).

Studies of stoichiometric $LiTMO_2$-type LMOs began in the 1950s, with a focus on the synthesis, structural identification, and examination of physical properties (colored with a blue gradient in Figure 1C). In 1956, Johnson and Heikes[20] first reported the $Li_xMn_{(1-x)}O$ system by sintering Li_2O_2 and MnO to construct a partial phase diagram. They further proposed the orthorhombic $LiMnO_2$ (*o*-$LiMnO_2$) and studied its magnetic properties. Later, owing to the capability of reversibly accommodating Li^+ ions, these materials have been studied as cathode materials (colored with an orange gradient in Figure 1C). In general, stoichiometric LMOs with an orthorhombic structure were more preferentially constructed than those with the layered structure using the usual methods, such as solid-state synthesis, which could be ascribed to the strong antiferromagnetic interactions between Mn^{3+} ions.[32,44] In 1996, the layered monoclinic $LiMnO_2$ (*m*-$LiMnO_2$) was synthesized using the ion exchange method from layered $NaMnO_2$.[10] Unfortunately, because of the severe structural change induced by the J–T effect, *m*-$LiMnO_2$ can hardly display the satisfied electrochemical performance. To stabilize the layered framework, heterogeneous elements can be incorporated into *m*-$LiMnO_2$ to form binary or ternary LMOs, such as $LiMn_xNi_{1-x}O_2$ and $LiMn_xNi_yCo_{1-x-y}O_2$ (NMCs). In particular, Ohzuku and Makimura[34] first developed $LiMn_{1/3}Ni_{1/3}Co_{1/3}O_2$, which combines the advantages of all TM activities and balanced stability, and thus offers a new direction for the development of commercial cathode materials.[35] Nowadays, NMCs have become one of the mainstream cathode material families. However, the large contents of elements other than Mn also introduce drawbacks, as described above. Recently, the *r*-Li–Mn–O cathode materials with microstructure design have been developed for high-performance LIBs.[19,36]

The Li-deficient LMOs were first studied at almost the same time as the stoichiometric $LiTMO_2$-type LMOs, including $LiMn_2O_4$, $LiMn_{1.5}Ni_{0.5}O_4$, etc., with a focus on the specific formulation as well as the crystallographic and magnetic properties.[23,24] The lack of efficient Li^+ ions leads to the generation of the more stable spinel structure instead of the layered structure. Later, these spinel materials were also used as cathode materials, which usually delivered better stability than the $LiTMO_2$-type LMOs.[25] Various optimization strategies, including doping, coating, surface/bulk structural regulations, and electrolyte modification, have been proposed to improve the electrochemical stabilities, working potentials, and energy densities for diverse spinel LMOs.[26,28–31] However, the capacities of LMOs are still limited because of the intrinsic deficiency of Li.

In contrast to the Li-deficient LMOs, the Li-rich LMOs were later found to exist when a portion of Li^+ ions occupy the TM sites in the stoichiometric $LiTMO_2$, which may maintain the pristine layered structure but break the original lattice symmetries. In particular, in the layered monoclinic Li_2MnO_3 (*m*-Li_2MnO_3, also formulated as $Li[Li_{1/3}Mn_{2/3}]O_2$), 1/3 Li^+ ions occupy the Mn sites and result in the $LiMn_2$ slab. The layered *m*-Li_2MnO_3 can be well integrated with the layered rhombohedral $LiTMO_2$,

yielding the Mn-based LLOs ($xLi_2MnO_3 \cdot (1-x)LiTMO_2$). These materials can deliver superior capacities owing to both the contributions from metal cationic redox (MCR) and oxygen anionic redox (OAR) accompanied by the activation of Li_2MnO_3, and their modification, such as by spinel incorporation, can significantly enhance the electrochemical stability. Due to the similar layered structures between Li_2MnO_3 and $LiTMO_2$, LLOs have complicated structures. The "twin domain" structures of LLOs have been well elucidated after long-term studies, which also suggests that Li_2MnO_3 and $LiTMO_2$ can present as different electrochemical functional units.[11,37–40] The attenuation of the J–T effect by tailoring the Mn^{3+}-related oxides is important for the optimization of LLOs, and the adjustment of the $Li_2MnO_3/LiTMO_2$ ratio provides a simple approach toward this goal. Furthermore, the full concentration gradient (FCG) design, based on tailoring the $Li_2MnO_3/LiTMO_2$ ratio in local regions, shows great opportunities for the optimization of electrochemical performance of LLOs.[41]

The J–T effect in LMLOs

The J–T effect was first proposed by H.A. Jahn and E. Teller in 1937.[45] This theorem demonstrates that, in the degenerated electron state, a non-linear molecule system will suffer from constant instability, and thus eliminate the degeneracy to form a new system with reduced symmetry and lower energy. In the non-linear fields of octahedral MnO_6, Mn^{3+} normally exhibits a high-spin state with a very large magnetic moment and the collinear J–T ordering of MnO_2 slabs along the elongated axes, causing the strong J–T distortion (Figure 2A). Compared with Mn^{3+} cations, the collective J–T distortion is apparently absent in Ni and Co cations because of the zigzag J–T ordering of TMO_2 slabs along the elongated axes or the absent electron in e_g orbitals in the Ni–O and Co–O frameworks.[46,47] Considering the electronic structures, for 3*d* TMs, including Mn, the 3*d* orbitals are divided into doubly degenerate e_g orbitals, including $d_{x^2-y^2}$ and d_{z^2}, and triply degenerate t_{2g} orbitals, including d_{xy}, d_{xz}, and d_{yz} (Figure 2B). For the high-spin Mn^{3+} cation ($t_{2g}^3e_g^1$) in an octahedral coordination, only one electron will occupy one e_g orbital (e_g^1), leading to the asymmetric occupation state of e_g orbitals. The electrons distributed in $d_{x^2-y^2}$ and d_{z^2} orbitals will show different degrees of shielding effect on the Mn nuclei in different directions. In this configuration, the overall *d* orbitals no longer match with the O_h symmetry of the octahedra, leading to the instability of the central Mn^{3+} cation. To stabilize the Mn^{3+} cation, the two longitudinal Mn–O bonds in the octahedral MnO_6 are elongated, while the other four horizontal Mn–O bonds are shrunk, as shown in Figure 2A. Such a distortion causes the symmetry reduction of the MnO_6 octahedron from O_h to D_{4h}, accompanied with the elimination of degenerate orbitals, reduction of the system energy, and distortion of crystal structures.[44,48] Especially, for LMLOs containing high-spin Mn^{3+} ($t_{2g}^3e_g^1$) ions, the deficient electrochemical performance during cycling is often seen because of the J–T effect.

Compared with Mn^{2+} and Mn^{4+}, Mn^{3+} is unique in terms of the J–T effect owing to its configuration of *d* electrons. Taking Mn^{4+} for a comparison, the differential charge densities of the octahedral $Mn^{3+}O_6$ and $Mn^{4+}O_6$ calculated using the density functional theory (DFT) are shown in Figure 2C. In contrast to $Mn^{4+}O_6$, $Mn^{3+}O_6$ shows an occupied d_{z^2} orbital, as reflected by the yellow regions beside the central Mn^{3+} cation. This means that the high-spin Mn^{3+} can induce the J–T distortion, while the high-spin Mn^{4+} cannot. Therefore, the J–T effect is closely correlated with the high-spin Mn^{3+}, and thus one of the central points for the stabilization of LMOs is the elimination of the high-spin Mn^{3+} in electrochemical process.

Apparently, the control of the spin state (*S*) of Mn^{3+} cation provides an intrinsic strategy for the elimination of the J–T distortion and the stabilization of LMOs. For Mn^{3+},

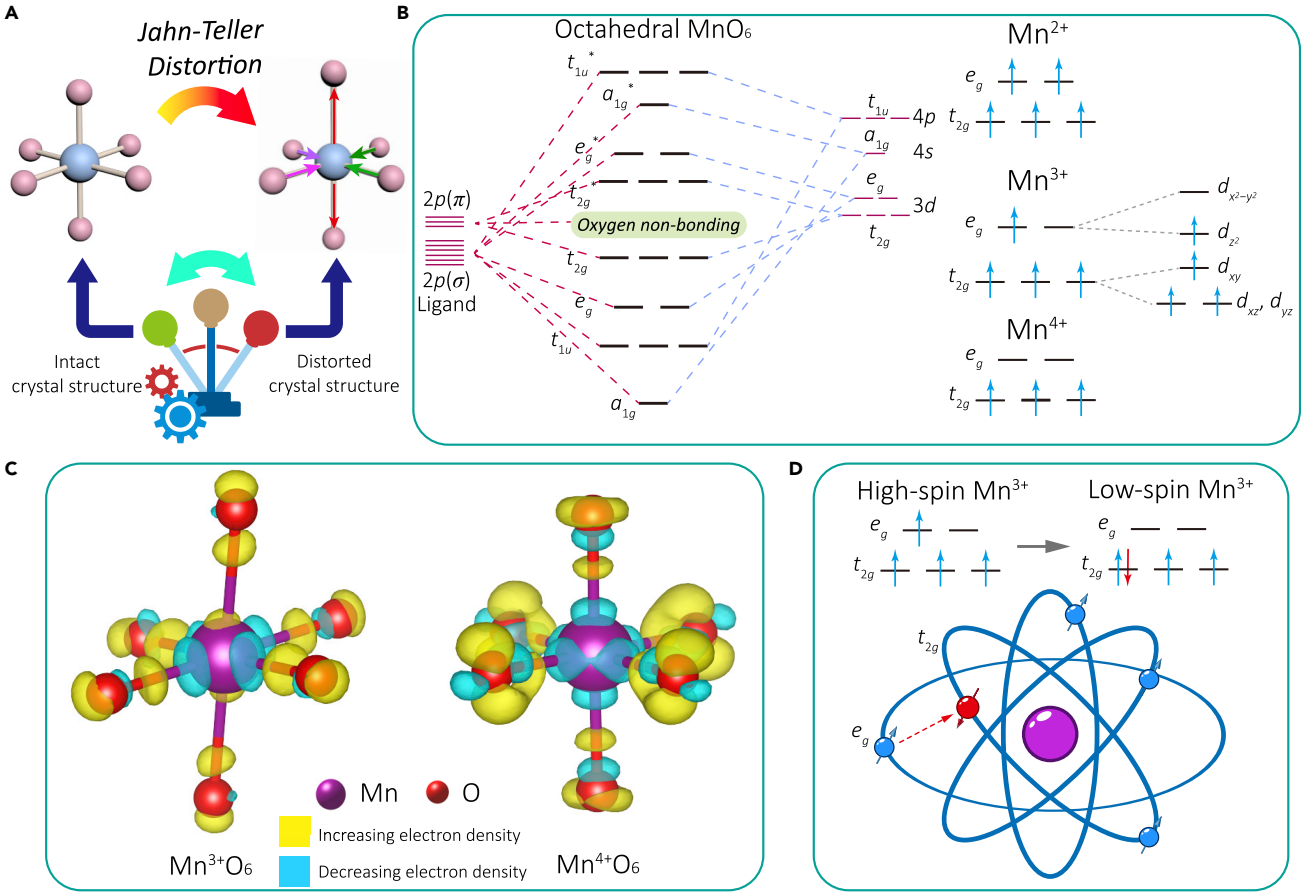

Figure 2. Schematic illustrations of the J–T effect in octahedral MnO_6

(A) A schematic of the octahedral MnO_6 before and after the J–T distortion.

(B) The molecular orbital energy diagram of the octahedral MnO_6 and the electronic orbitals of $Mn^{2+}/Mn^{3+}/Mn^{4+}$ ions.

(C) The calculated differential charge densities of the octahedral $Mn^{3+}O_6$ and $Mn^{4+}O_6$. Blue and yellow regions represent the decreasing and increasing electron density, respectively. The iso-surface of the charge density is set as 0.015 e/Bohr.[3]

(D) Schematic diagrams of Mn 3*d* orbitals with high-/low-spin Mn^{3+} ions.

two spin configurations could be hypothesized in the rhombohedral $LiMnO_2$ (*r*-$LiMnO_2$) phase, including high-spin ($t_{2g}^3e_g^1$, $S = 2$) and low-spin ($t_{2g}^4e_g^0$, $S = 1$) states. In particular, under the low-spin state, the electrons of Mn^{3+} occupy all t_{2g} levels with a spin-down electron (Figure 2D), resulting the inactivity of the J–T effect of Mn^{3+} in *r*-$LiMnO_2$.[49,50] Moreover, by introducing different ligands into the Mn coordination system, the low-spin Mn^{3+} complexes can be fabricated.[51] Very recently, the microstructure design has provided new insights into the elimination of the J–T effect for a $LiMnO_2$ cathode.[19] The interfacial orbital ordering, with the d_{z^2} orbitals of the spinel and layered crystal domains being perpendicular, could disrupt the long-range orbital ordering, which significantly reduces the J–T effect.

Spinel Li-, Mn-based oxides

In 1983, the Mn-based cubic spinel $LiMn_2O_4$ (Figure 3A), with a space group of $Fd\bar{3}m$, was first used as a cathode material in LIBs by Thackeray et al.[25] The general formula of spinel AB_2X_4 can be drawn from $LiMn_2O_4$, in which the alkali cation A fills one-eighth of the tetrahedral sites (8a), the TM cation B fills half of the octahedral sites (16d), and the anion X (O in spinel LMOs) fills the 32e sites to form a cubic close packed (ccp) array. In $LiMn_2O_4$, the crosslinking interstitial octahedral 16c sites

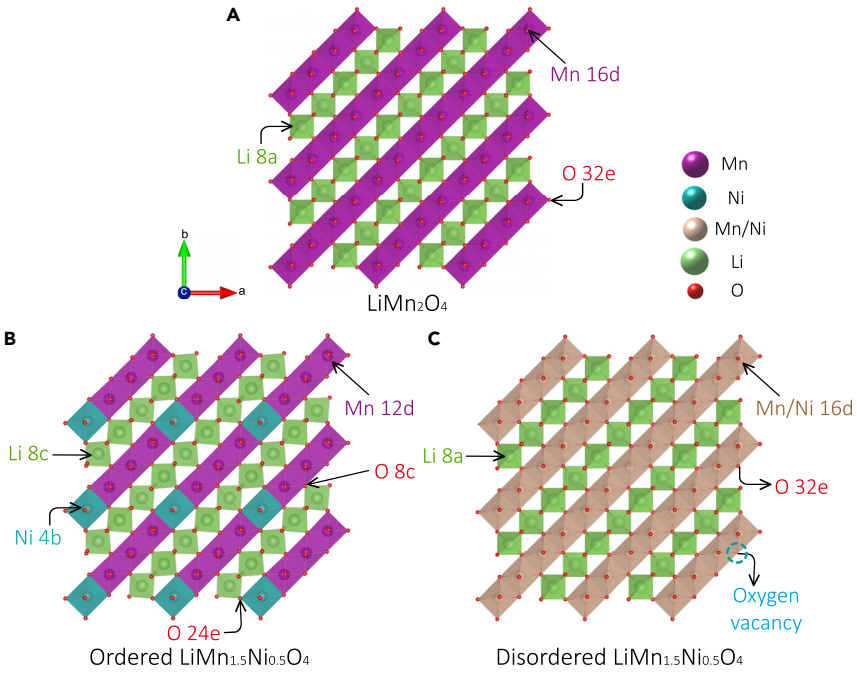

Figure 3. Schematic illustrations of crystal structures of representative Li-, Mn-based spinels
(A) $LiMn_2O_4$.
(B) Ordered $LiMn_{1.5}Ni_{0.5}O_4$.
(C) Disordered $LiMn_{1.5}Ni_{0.5}O_4$.

provide three-dimensional channels as Li^+ diffusion pathways, allowing Li^+ cations to hop from 8a to 16c to 8a sites. $LiMn_2O_4$ exhibits a theoretical capacity of 148 mAh g^{-1} at voltages between 3.0 and 4.3 V, with a specific energy density of ~490 Wh kg^{-1}. The average valence of Mn in $LiMn_2O_4$ is +3.5, which is a critical point for the J–T effect since half of Mn ions are Mn^{3+} ($t_{2g}^3e_g^1$).[52] During the $Mn^{3+/4+}$ redox process during electrochemical (de)lithiation, the structural degradation of spinel LMOs between the cubic $LiMn_2O_4$ and tetragonal $Li_2Mn_2O_4$ can take place.[53,54]

The J–T active Mn^{3+} cations can undergo the disproportionation reaction of $2Mn^{3+} \rightarrow Mn^{4+} + Mn^{2+}$, which is also a crucial reason for the structure and capacity degradation of spinel $LiMn_2O_4$. During cycling, H^+ and F^- ions dissociated from the strong Lewis acid HF by-product of electrolytes would react with active axial oxygen species and TM ions to form H_2O and fluoride species, respectively.[55,56] Simultaneously, electrons will transfer from the metal to the ligand, and thus the J–T active Mn^{3+} is oxidized to Mn^{4+}. The reduction of other Mn^{3+} ions to J–T-free Mn^{2+} ions causes the instantaneous oxidization of electrolytes, evolution of gases, and generation of other reactive protic species. Moreover, the Mn^{2+} ions can easily dissolve into the electrolyte and deposit onto the negative electrode, leading to the gradual degradation of the spinel cathode $LiMn_2O_4$.[55,57,58]

To decrease the contents of bulk J–T-active Mn^{3+} ions, different spinel derivatives on the basis of $LiMn_2O_4$ have been developed. One of the most popular derivatives is the high-voltage $LiMn_{1.5}Ni_{0.5}O_4$ (LMNO) spinel by introducing the low-valence Ni^{2+} into the parent spinel. As a result, the valence of Mn cations may be increased to +4, which may inhibit the J–T effect of the material.[27,59] However, it should be noted that such a strategy is influenced by the crystal structures of LMNO. In general, two

different structures of LMNO, including the ordered ($P4_332$) and disordered ($Fd\bar{3}m$) structures according to the locations of TMs (Figures 3B and 3C), can be obtained by different sintering temperatures. Moderate temperatures of ~700°C are suitable for the formation of the ordered phase. In contrast, elevated temperatures stimulate the formation of disordered phase due to the oxygen loss in the bulk phase, which causes the charge compensation by the partial reduction of Mn^{4+} to the J–T active Mn^{3+}.[60] Although the Mn^{3+} cations can enhance the superb electronic conductivity, discharge capacity, and rate performance of the disordered LMNO, the existing J–T distortion still hampers the structural stability and cycle performance. Bulk doping could be one effective solution to suppress the J–T distortion. For example, Mg^{2+} distributed at the tetrahedral 8a and octahedral 16c sites of LMNO could reduce the two-phase reaction from $Li_{0.5}Ni_{0.5}Mn_{1.5}O_4$ to $Ni_{0.25}Mn_{0.75}O_2$ and create exceptional cycle stability.[61]

However, normal spinel LMOs could not sustain enough capacity and energy density due to the deficient Li^+ ions,[31] and new design of spinel LMOs based on the adjustment of the local Mn–O structure is required. From the direction shown in Figure 3, the spinel phase could display a partially layered structure, with tetrahedral Li^+ occupancies instead of edge-shared octahedral configurations. Moreover, the lithiated spinel $Li_2Mn_2O_4$ can deliver a capacity of nearly 300 mAh g^{-1} due to the two-Li^+ (de)intercalation.[25,53] Nevertheless, the existing issues, including the phase transition/separation and J–T effect-induced structural degradation, could not be avoided. An effective way to address these problems for the fabrication of high-quality spinels could be the design of face-shared tetrahedral and octahedral structures and disordered cationic lattices, which favors the high mobility of Li^+ ions and thus better performances.[31,62,63]

Lithium-rich, manganese-based layered oxides

Because of the eminent properties of LMLOs, researchers persevered in developing and optimizing these materials with stable structures and enhanced performances. One of the effective ways is the incorporation of electrochemical inactive functional units to suppress the structural degradations during electrochemical cycling. In particular, Thackeray and colleagues[11,37] first adopted a chemical acid leaching method for the defective spinel λ-MnO_2 to fabricate $Li_{2-x}MnO_{3-x/2}$ ($0 < x < 2$) with a ccp oxygen array. A lithiated derivative oxide $Li_{1.09}Mn_{0.91}O_2$ ($0.2Li_2MnO_3 \cdot 0.8LiMnO_2$) was thus obtained, which could be nominated as the predecessor of LLOs ($xLi_2MnO_3 \cdot (1-x)LiTMO_2$). In LLOs, both the randomly distributed Li_2MnO_3-like crystal domain and the intergrown $LiTMO_2$ crystal domain exist in the lattice. Thus, LLOs can be interpreted as "twin domain" structured materials. The crystal domains evolve under the influence of electrochemical operations and environmental conditions, such as the cutoff voltages and activation temperatures, showing strong synergistic effects and interconversions.[64] Benefiting from the Li_2MnO_3-like crystal domain, LLOs are more stable than $LiTMO_2$ alone during electrochemical (de)lithiation processes below 4.4 V versus Li/Li^+. Surprisingly, the Li_2MnO_3-like crystal domain can be activated at voltages above 4.4 V, a process correlated with activation of the OAR process. OAR can provide considerable capacity with the increase of activation depth. Therefore, the reaction mechanisms of LLOs can be briefly concluded as being the co-existence of MCR and OAR during electrochemical processes (Figure 4A).[65] Therefore, although most of the average voltages of LMOs are lower than Ni/Co-based layered oxide cathodes, Mn-based LLOs can deliver a high capacity of >250 mAh g^{-1} with an average voltage of ~3.6 V, which still makes the LMLOs one of the most important cathode families for the next-generation high-energy LIBs.[2,39,66] However, LLOs suffers from diverse drawbacks, such as the poor rate

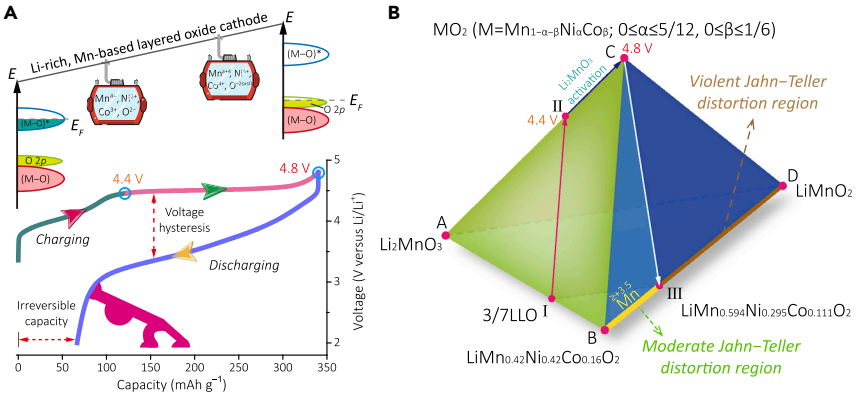

Figure 4. Schematic illustrations of the redox mechanism and reaction routes in LLOs
(A) Schematic of MCR and OAR in the initial (de)lithiation process of LLOs.
(B) Three-dimensional quaternary reaction route diagram of LLOs with regions of different degrees of J–T effect.

performance, large voltage hysteresis, and serious voltage degradation during electrochemical cycling. These drawbacks have been partially eliminated by continuous progress.[2,41,56,66,67]

As a member of the LMLOs, *m*-Li_2MnO_3 with a space group of *C*2/*m* has a similar structure to *r*-$LiTMO_2$, in which 1/3 TM sites are occupied by Li^+ ions, leading to the formation of the honeycomb $LiMn_2$ superstructure. Although the Li_2MnO_3-like crystal domain in LLOs could stabilize the $LiTMO_2$ structure, Mn^{3+} ions in $LiTMO_2$ can still generate the J–T effect and induce a large volumetric strain for the bulk, which reduces the electrochemical reversibility because of the repeated volume variation and possible formation of cracks. Furthermore, due to the occupation of Li^+ ions in the TM layers, the Li–O–Li configurations appear in the LLO structures, inducing the formation of a non-bonding-like O orbital, which locates near the Fermi level and thus makes electron loss from O (OAR) quite possible.[68] Thus, the OAR occurring in LLOs at high potentials can provide extra capacity; however, the lattice O can easily escape from the LLO surface, causing a decrease of the average valence of Mn and thus more obvious J–T effect.[41,69] At the same time, the O vacancies decrease the migration energy barrier of Mn and lattice densification of bulk LLO. The proper design of the bulk structure intrinsically alters the properties of LLOs for better electrochemical performance.

To discern the relationships between the structural evolution of LLOs and their design, and to consider the compositions of Li_2MnO_3-like and $LiTMO_2$ crystal domains, the crystal-domain reaction mechanism of LLOs was proposed, as shown in the three-dimensional quaternary reaction route diagram (Figure 4B). In this diagram, the two electrochemical stages (<4.4 V and 4.4–4.8 V) determined by the reactions of $LiTMO_2$- and Li_2MnO_3-like crystal domains, respectively, can be clearly observed. Moreover, based on the evolved structures of LLOs with different components in this diagram, the regions of J–T distortion with different degrees can be outlined by the valences of Mn.

We take $Li_{1.13}Mn_{0.517}Ni_{0.256}Co_{0.097}O_2$ ($0.3Li_2MnO_3 \cdot 0.7LiMn_{0.42}Ni_{0.42}Co_{0.16}O_2$, 3/7LLO) as a typical LLO material to explore the underlying reaction mechanisms. After the initial full activation process (line I–II, II–C, and C–III), the majority of components are transformed into the monoclinic $LiTMO_2$ structure (point III). In the

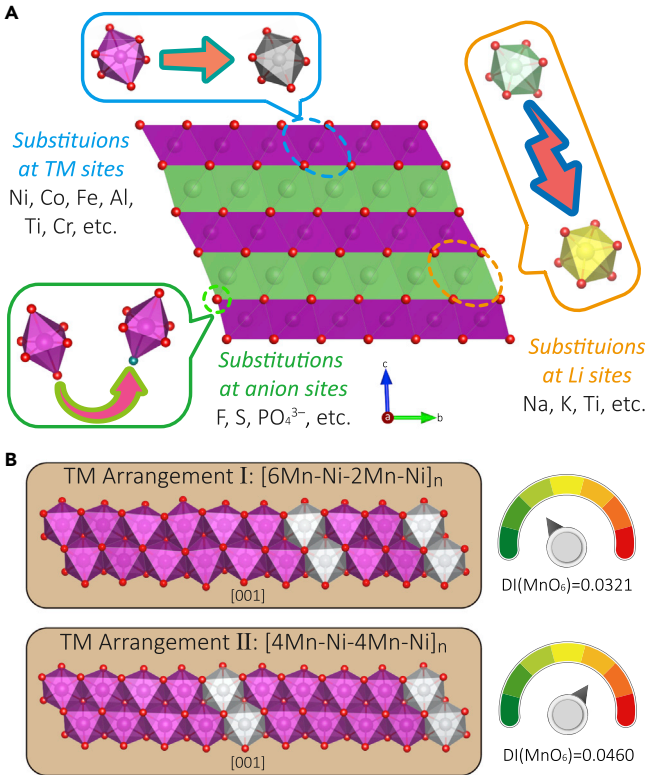

Figure 5. Schematic illustrations of strategies to prevent the J–T effect

(A) Schematic of bulk elemental substitution/doping strategies in LMLOs.

(B) TM (Mn and Ni) arrangements in the TM layer of the representative $LiMn_{0.8}Ni_{0.2}O_2$.

following cycles, Mn dominates the major capacity contribution of MCR.[64,66] When MCR dominates the electrochemistry during (de)lithiation processes, the J–T effect plays a detrimental role in the average and local structures due to the formation of Mn^{3+} cations. The average valence of Mn in 3/7LLO after full activation should be +3.5, which is the critical point for the J–T effect.[52,66] With the appropriate increase of the $LiTMO_2$ fraction, owing to the rising valence of Mn after the initial activation cycle, better structural and cyclic stability could be acquired. Hence, the well-designed LLO pristine materials with diminishing J–T effect interference (the valence of Mn above +3.5 after the first cycle) and controlling the degree of OAR (by controlling the activation degree of Li_2MnO_3) could show highly optimized electrochemical properties.

Remedies for J–T distortion in LMLOs

Aside from the strategy of tuning crystal-domain compositions and electronic structures, many other strategies have been proposed to inhibit the J–T distortion for stable cathode materials for a long time. One of the commonly used strategies is the bulk elemental substitution/doping in LMLOs. According to the substitution/doping sites, including TM, Li, and O, three types of dopants can be concluded (Figure 5A). The popular dopants at TM sites include Ni, Co, Fe, Al, Ti, Mg, and Cr, yielding many TM-substituted/doped compounds from the parent $LiMnO_2$, such as $LiMn_{0.5}Ni_{0.5}O_2$ and $LiMn_{0.9}Co_{0.1}O_2$.[13–15,18,33,70–72] These dopants can either alter the neighboring atomic structures of Mn ions, resulting in more stable average structures than that of the pristine materials or directly tune the valence of Mn to a level above +3.5 to avoid

the violent J–T regions, such as introducing low-valence elements, Mg^{2+}/Ni^{2+}, into the bulk phase.[73] Introducing Na, K, and Ti dopants into the Li sites of layered structure can also enhance the structural stability, because the large dopants in the Li layer may adjust the bond lengths to be uniform, thereby maintaining the symmetry of MnO_6 octahedra.[70,74,75] Doping with anionic species at the O sites of MnO_6 is also promising due to the variant covalency of Mn–X interactions (X = F^-, S^{2-}, and PO_4^{3-}, etc.), which is ascribed to their different electronegativities and radii, so that the distortion of MnO_6 octahedra could be inhibited.[16,76,77]

Moreover, the arrangement of TM cations in the TM layer of LMLOs is also crucial to tailor the crystal structures and electrochemical properties. In 2007, Thackeray et al.[78] proposed the cation arrangements of the flower-like $LiMn_{6-x}M_x$ (M = Ni, Co) in the TM layers of LMLOs, such as $LiMn_6$ and $LiMn_5Ni$ cation ordering units in the Li_2MnO_3-like and $LiMn_{0.5}Ni_{0.5}O_2$ units, respectively. Heterogeneous ions would disturb the regular arrangements of TMs and their neighbor structures. Therefore, the electronic interactions affect the charge ordering, which would influence the electrochemical behaviors.

By selecting $LiMn_{0.8}Ni_{0.2}O_2$ as a model material, we tentatively investigated the relationship between the arrangement of TMO_6 (MnO_6 and NiO_6 octahedra) in TM layers and the J–T effect in LMLOs. Two different TM arrangement types, including $[6Mn\text{-}Ni\text{-}2Mn\text{-}Ni]_n$ and $[4Mn\text{-}Ni\text{-}4Mn\text{-}Ni]_n$, were designed, as shown in Figure 5B. We refer to the distortion index DI(MnO_6) to reflect the degree of J–T distortion in MnO_6 octahedra, which is defined as follows:[79]

$$DI(MnO_6) = \frac{1}{6}\sum_{i=1}^{6}\frac{|d_i - d_{ave}|}{d_{ave}}$$

where d_i and d_{ave} demonstrate the specific and average Mn–O bond length, respectively. In Figure 5B, DI(MnO_6) values of the two TM arrangements are calculated to be 0.0321 and 0.0460, respectively (Figures S1 and S2). The lattice constant of TM arrangement II is more similar to the $R\bar{3}m$ symmetry than that of TM arrangement I (see Table S1 and Figures S1 and S2), which means that the $[6Mn\text{-}Ni\text{-}2Mn\text{-}Ni]_n$ arrangement has a higher structure symmetry. Therefore, the architecture of TM arrangement II shows less influence on the lattice intactness than that of TM arrangement I. In terms of the matching degree of lattice, the different distributions of NiO_6 octahedra in the TM layer would lead to different MnO_6 octahedral symmetries. In other words, the introduction of Ni at diverse sites of TM layers could suppress the extension of the Mn–O bond length. From the theoretical speculations, distinguished crystal structures and arrangements of TM ions could be beneficial to prevent J–T distortion, which could be realized by designing and tailoring the synthetic conditions, processes, and technologies, such as the type of TM ions, thermal treatment temperatures, and procedures selected. This proposition holds considerable opportunities for further improvements of versatile J–T-inhibited LMLOs, which would be more beneficial to enhance the electrochemical performances and large-scale use of the LMLOs.

Synthesis strategies of LMLOs for suppressing the J–T effect

The prevailing synthetic strategies of LMLOs include the co-precipitation, ion exchange, solid-state synthesis, high-pressure synthesis, and sol-gel and solvothermal methods, which show diverse advantages (Figure 6).[36,40,72,80,81] The co-precipitation is the most popular method to synthesize commercial cathode materials, which

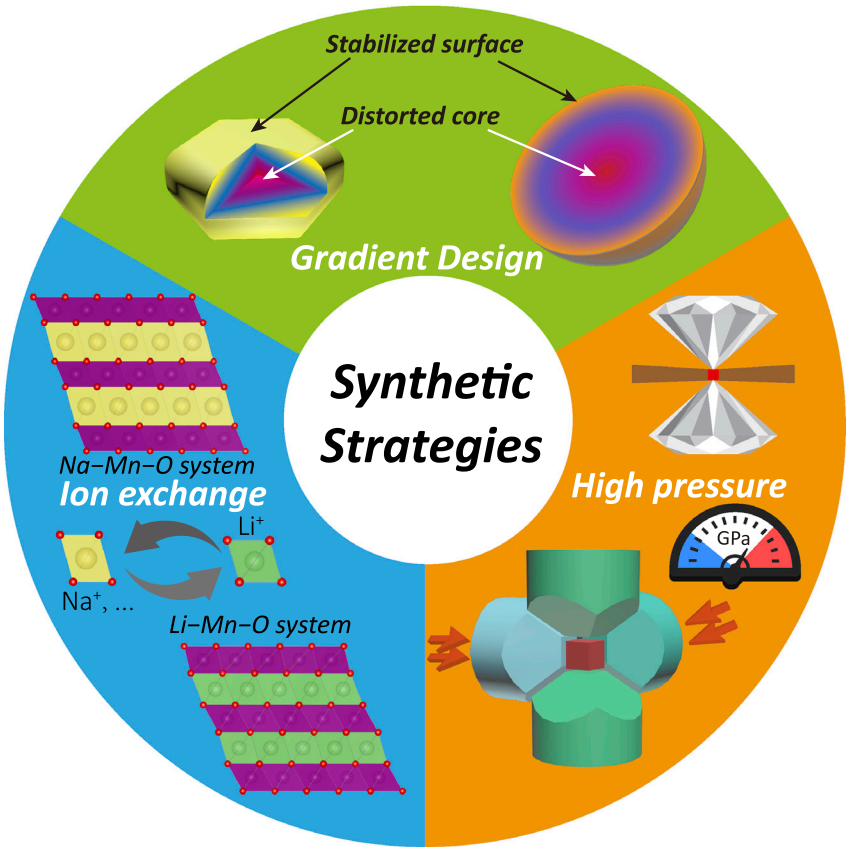

Figure 6. Schematic illustrations of synthesis strategies of LMLOs for the suppression of the J–T effect

can easily tailor the chemical compositions, particle sizes, morphologies of agglomerates, and "single-crystal" particles.[41,80] In addition, FCG design through co-precipitation was first exploited in Ni-rich layered oxides, showing high energy density, high thermal stability, and durable cycle life, using the optimized gradient design.[35] Recently, the gradient design was also been realized in Mn-based LLOs. Among a series of FCG-tailored structural designs, different gradient slopes of linearly decreasing Mn and increasing Ni and Co from the interior to the exterior of the agglomerated spheres show suppressed voltage decay, improved electrochemical performances, and enhanced thermal stability.[41] This strategy can reduce the J–T effect because the lattice-stabilized 3/7 LLO is fabricated at the particle surface and the valences of Mn ions can be tailored by the proportion and composition of crystal domains. In addition to the agglomerated spherical LLOs, single-crystal LLOs also show promise, since their mechanical behavior, and thermal and interface stability, are clearly enhanced over their agglomerate analogs.[80,82] Combining the FCG design with single-crystal particle configuration, optimized overall electrochemical performances are expected in the future.

The layered $LiMnO_2$ with a monoclinic phase and *C*2/*m* space group of α-$NaFeO_2$ structure was first prepared by Armstrong and Bruce[10] in 1996 by ion exchange from the layered $NaMnO_2$, which shed light on the low-cost and high-energy-density LMLO cathode materials for LIBs. In general, the stoichiometric $LiMnO_2$ prepared by solid-state synthesis is always in the orthorhombic phase with a space group of

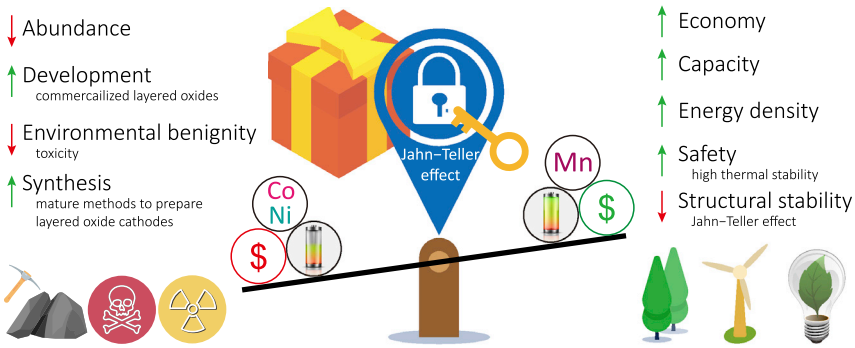

Figure 7. Trade-offs of LMLOs and other TM-based layered cathodes

Pmnm, exhibiting a distorted ccp oxygen anion array in the ordered-rocksalt structure because the octahedral LiO_6 and MnO_6 units arrange in the zigzag Li and Mn layers, respectively. Compared with the *C*2/*m* symmetry, the $R\bar{3}m$ symmetry in the Li–Mn–O system has higher structural reversibility and faster Li^+ migrating characteristics. Although the synthesis procedure is complicated by exchanging Na^+ with Li^+ cations, the recently reported Li-rich *r*-$Li_{0.91}Mn_{0.76}O_2$ still shows impressive rate performances.[80] At the same time, the Mn ions show a low-spin state in the pristine materials, which can mitigate the structural distortion and degradation caused by the J–T effect. Recently, accompanied by the OAR, the high-capacity and high-energy-density properties of LMLOs were also realized by this strategy, attracting more and more researchers to fabricate high-performance and low-cost LMLO cathodes.[40,83,84] Hitherto, proposals to address the J–T effect of Mn^{3+} in layered $LiMnO_2$, and to synthesize the rhombohedral phase with a space group of $R\bar{3}m$ in a facile and efficient way, are still challenging.

The Mn–O bond lengths in the rhombohedral symmetry of $LiMnO_2$ have been indicated to be equal.[81,85] To handle the J–T effect of Mn^{3+}-containing MnO_6 octahedra, the high-pressure synthesis may show advantages to suppress the distortion and to fabricate the rhombohedral phase spontaneously. The high-pressure and high-temperature environment could reduce the lengths of the two elongated Mn–O bonds in the MnO_6 octahedra and contribute to the higher energy barrier of MnO_6-octahedra structural rearrangement, showing a unique way to eliminate the J–T distortion.[86,87] For example, by using Co substitution, the lattice of the *r*-$LiMnO_2$ matrix can be stabilized in the high-pressure and high-temperature environment to form *r*-$LiMn_{0.36}Co_{0.64}O_2$ with no J–T behavior and high-energy-density performance.[81] However, the economic and industrial advantages of LMLOs prepared using this strategy are decreased because of the existence of electrochemical inactive phases and the large amount of Co participation. Therefore, optimization of the high-pressure method is needed to further develop LMLOs as cathode materials with high Mn content to eliminate the J–T distortion.

Conclusions and outlook

Because of the historical progress and experience in structural design, LMLOs have become important among various energy storage materials and are expected to be revived in future (Figure 7). Currently, the imperative task for their practical applications is to find highly efficient methods to develop J–T-free LMLO cathode materials, which need to have high structural stability, suppressed layer-to-spinel transition, superior long cycle life, and negligible voltage decay.[19]

The regulation of Mn valence throughout the electrochemical cycling process is of primary importance to avoid the violent J–T effect and to suppress structural distortion. To this end, one of the effective methods is the substitution/doping of heterogeneous atoms in bulk to increase the average valence of Mn. First, the introduction of vacancies of Mn or O ions may also be effective to control the J–T distortion by restraining the elongated bonds and tuning the valence of Mn ions.[88] Second, various components with different ratios could be integrated to tune the Mn valence. In particular, the valence of Mn in LLOs after the initial activation process can be tailored by the proportion of $LiTMO_2$- and Li_2MnO_3-like crystal domains.[66] Third, the stabilization of the metastable structure by external stimuli is unique to obtain specific LMLOs. For example, under the high-pressure and/or high-temperature environment, the lengths of chemical bonds can be altered, and thus symmetry of the octahedral MnO_6 can be directly enhanced.[81] The mismatching pressure from specific epitaxial orientation growth in the thin-film cathode materials could also selectively tailor the Mn–O bonds and thus obtain high symmetry.[50] Finally, the localized structure design has also shown notable effectiveness, which can confine the distortion units in localized regions with short-range ordering.[19,41,66] In particular, the design of FCG-tailored Mn-based LLOs with agglomerated and single-crystal structures is a unique and effective method, which can combine the advantages of different microstructures at different particle regions.[41]

At present, in the representative LMLO system, stabilizing the crystal structures of the pristine and electrochemical dynamic states is a highly challenging issue to be addressed to meet the ever-increasing demands of advanced cathode materials for LIBs. The irreversible structural degradation from layered structures to spinel and rocksalt structures, dissolution of the elements, the large volume deformation during (de)lithiation processes, as well as the J–T effect resulting from Mn^{3+} cations, are issues that need to be resolved as soon as possible. With the deepening of the understanding of the properties and structures of LMLO systems, new views and solutions to enhance the electrochemical performances could be advanced by the design of functional units with specific architectures. Coping with the J–T effect will remain of key importance in the materials design, including the localized structures and microstructures, which could be realized by tailoring the crystal domains and electronic states. All in all, we stand at a turning point in history with great opportunities, huge potentials, and urgent demands for the revival of the use of LMLOs. Once the J–T effect is addressed properly, we foresee the practical values of LMLOs in general.

METHODS

The DFT calculations were performed using the Vienna Ab initio Simulation Package.[89,90] The electron exchange and correlation energy were treated within the generalized gradient approximation in the Perdew-Burke-Ernzerhof functional. The kinetic energy cutoff of the plane-wave basis was 480 eV. The Brillouin zone was sampled at the Γ-point for 10a × 1b × 1c supercell (contains 30 $LiTMO_2$ units). The force on each atom in the optimized geometry was less than 0.05 eV $Å^{-1}$ and the energy was less than 10^{-5} eV between two consecutive steps, when assuming U values for Mn and Ni of 4.9 and 6.0, respectively.

SUPPLEMENTAL INFORMATION

Supplemental information can be found online at https://doi.org/10.1016/j.matt.2021.02.023.

ACKNOWLEDGMENTS

S.Q.L. thanks Mr. Tianhao Wu and Mr. Yinzhong Wang for their worthwhile discussions by telecommuting during the COVID-19 pandemic period. This work was financially supported by the Beijing Natural Science Foundation (grant nos. JQ19003 and KZ202010005007), the National Natural Science Foundation of China (grant nos. 21975006 and U19A2018).

AUTHOR CONTRIBUTIONS

Conceptualization, H.J.Y.; investigation, S.Q.L., B.Y.W., S.Z., and Z.H.Z.; writing – original draft, S.Q.L. and B.Y.W.; writing – review & editing, S.Q.L., X.Z., and H.J.Y.; supervision, H.J.Y.

DECLARATION OF INTERESTS

The authors declare no competing interests.

REFERENCES

1. Goodenough, J.B., and Park, K.S. (2013). The Li-ion rechargeable battery: a perspective. J. Am. Chem. Soc. *135*, 1167–1176.
2. Yu, H., and Zhou, H. (2013). High-energy cathode materials (Li_2MnO_3-$LiMO_2$) for lithium-ion batteries. J. Phys. Chem. Lett. *4*, 1268–1280.
3. Manthiram, A. (2020). A reflection on lithium-ion battery cathode chemistry. Nat. Commun. *11*, 1550.
4. Liang, Y., Zhao, C.Z., Yuan, H., Chen, Y., Zhang, W., Huang, J.Q., Yu, D., Liu, Y., Titirici, M.M., Chueh, Y.L., et al. (2019). A review of rechargeable batteries for portable electronic devices. InfoMat *1*, 6–32.
5. Li, F., Li, J., Zhu, F., Liu, T., Xu, B., Kim, T.-H., Kramer, M.J., Ma, C., Zhou, L., and Nan, C.-W. (2019). Atomically intimate contact between solid electrolytes and electrodes for Li batteries. Matter *1*, 1001–1016.
6. Yoon, C.S., Jun, D.-W., Myung, S.-T., and Sun, Y.-K. (2017). Structural stability of $LiNiO_2$ cycled above 4.2 V. ACS Energy Lett. *2*, 1150–1155.
7. Kim, U.-H., Kuo, L.-Y., Kaghazchi, P., Yoon, C.S., and Sun, Y.-K. (2019). Quaternary layered Ni-rich NCMA cathode for lithium-ion batteries. ACS Energy Lett. *4*, 576–582.
8. Nam, G.W., Park, N.-Y., Park, K.-J., Yang, J., Liu, J., Yoon, C.S., and Sun, Y.-K. (2019). Capacity fading of Ni-rich NCA cathodes: effect of microcracking extent. ACS Energy Lett. *4*, 2995–3001.
9. Bianchini, M., Roca-Ayats, M., Hartmann, P., Brezesinski, T., and Janek, J. (2019). There and back again-the journey of $LiNiO_2$ as a cathode active material. Angew. Chem. Int. Ed. *58*, 10434–10458.
10. Armstrong, A.R., and Bruce, P.G. (1996). Synthesis of layered $LiMnO_2$ as an electrode for rechargeable lithium batteries. Nature *381*, 499–500.
11. Thackeray, M.M., and Rossouw, M.H. (1991). Lithium manganese oxides from Li_2MnO_3 for rechargeable lithium battery applications. Mat. Res. Bull. *26*, 463–473.
12. Deng, Z.Q., and Manthiram, A. (2011). Influence of cationic substitutions on the oxygen loss and reversible capacity of lithium-rich layered oxide cathodes. J. Phys. Chem. C *115*, 7097–7103.
13. Nayak, P.K., Grinblat, J., Levi, M., Levi, E., Kim, S., Choi, J.W., and Aurbach, D. (2016). Al doping for mitigating the capacity fading and voltage decay of layered Li and Mn-rich cathodes for Li-ion batteries. Adv. Energy Mater. *6*, 1502398.
14. Wang, Y.X., Shang, K.H., He, W., Ai, X.P., Cao, Y.L., and Yang, H.X. (2015). Magnesium-doped $Li_{1.2}[Co_{0.13}Ni_{0.13}Mn_{0.54}]O_2$ for lithium-ion battery cathode with enhanced cycling stability and rate capability. ACS Appl. Mater. Interfaces *7*, 13014–13021.
15. Billaud, J., Sheptyakov, D., Sallard, S., Leanza, D., Talianker, M., Grinblat, J., Sclar, H., Aurbach, D., Novák, P., and Villevieille, C. (2019). Li/Fe substitution in Li-rich Ni, Co, Mn oxides for enhanced electrochemical performance as cathode materials. J. Mater. Chem. A *7*, 15215–15224.
16. Li, L., Song, B.H., Chang, Y.L., Xia, H., Yang, J.R., Lee, K.S., and Lu, L. (2015). Retarded phase transition by fluorine doping in Li-rich layered $Li_{1.2}Mn_{0.54}Ni_{0.13}Co_{0.13}O_2$ cathode material. J. Power Sources *283*, 162–170.
17. Jang, Y.-I., Huang, B., Chiang, Y.-M., and Sadoway, D.R. (1998). Stabilization of $LiMnO_2$ in the α-$NaFeO_2$ structure type by $LiAlO_2$ addition. J. Electrochem. Soc. *1*, 13–16.
18. Armstrong, A.R., Robertson, A.D., Gitzendanner, R., and Bruce, P.G. (1999). The layered intercalation compounds $Li(Mn_{1-y}Co_y)O_2$: positive electrode materials for lithium-ion batteries. J. Solid State Chem. *145*, 549–556.
19. Zhu, X., Meng, F., Zhang, Q., Xue, L., Zhu, H., Lan, S., Liu, Q., Zhao, J., Zhuang, Y., Guo, Q., et al. (2020). $LiMnO_2$ cathode stabilized by interfacial orbital ordering for sustainable lithium-ion batteries. Nat. Sustain. https://doi.org/10.1038/s41893-41020-00660-41899.
20. Johnston, W.D., and Heikes, R.R. (1956). A study of the $Li_xMn_{(1-x)}O$ system. J. Am. Chem. Soc. *78*, 3255–3260.
21. Dittrich, G., and Hoppe, R. (1969). Zur Kristallstruktur von $LiMnO_2$. Z. Anorg. Allg. Chem. *368*, 262–270.
22. Hoppe, R., Brachtel, G., and Jansen, M. (1975). Zur Kenntnis der Oxomanganate(III): Über $LiMnO_2$ und β-$NaMnO_2$. Z. Anorg. Allg. Chem. *417*, 1–10.
23. Wickham, D.G., and Croft, W.J. (1958). Crystallographic and magnetic properties of several spinels containing trivalent manganese. J. Phys. Chem. Sol. *7*, 351–360.
24. Blasse, G. (1966). Ferromagnetism and ferrimagnetism of oxygen spinels containing tetravalent manganese. J. Phys. Chem. Sol. *27*, 383–389.
25. Thackeray, M.M., David, W.I.F., Bruce, P.G., and Goodenough, J.B. (1983). Lithium insertion into manganese spinels. Mat. Res. Bull. *18*, 461–472.
26. Tarascon, J.M., Wang, E., Shokoohi, F.K., McKinnon, W.,R., and Colson, S. (1991). The spinel phase of $LiMn_2O_4$ as a cathode in secondary lithium cells. J. Electrochem. Soc. *138*, 2859.
27. Amine, K., Tukamoto, H., Yasuda, H., and Fuiita, Y. (1996). A new three-volt spinel $Li_{1+x}Mn_{1.5}Ni_{0.5}O_4$ for secondary lithium batteries. J. Electrochem. Soc. *143*, 1607–1613.
28. Amatucci, G.G., Blyr, A., Sigala, C., Alfonse, P., and Tarascon, J.M. (1997). Surface treatments of $Li_{1+x}Mn_{2-x}O_4$ spinels for improved elevated temperature performance. Solid State Ionics *104*, 13–25.
29. Chemelewski, K.R., Lee, E.-S., Li, W., and Manthiram, A. (2013). Factors influencing the electrochemical properties of high-voltage spinel cathodes: relative impact of morphology and cation ordering. Chem. Mater. *25*, 2890–2897.
30. Chen, L., Fan, X., Hu, E., Ji, X., Chen, J., Hou, S., Deng, T., Li, J., Su, D., Yang, X., et al. (2019). Achieving high energy density through increasing the output voltage: a highly reversible 5.3 V battery. Chem *5*, 896–912.

31. Ji, H., Wu, J., Cai, Z., Liu, J., Kwon, D.-H., Kim, H., Urban, A., Papp, J.K., Foley, E., Tian, Y., et al. (2020). Ultrahigh power and energy density in partially ordered lithium-ion cathode materials. Nat. Energy *5*, 213–221.

32. Ohzuku, T., Ueda, A., and Hirai, T. (1992). $LiMnO_2$ as cathode for secondary lithium cell. Chem. Express *7*, 193.

33. Rossen, E., Jones, C.D.W., and Dahn, J.R. (1992). Structure and electrochemistry of $Li_xMn_yNi_{1-y}O_2$. Solid State Ionics *57*, 311–318.

34. Ohzuku, T., and Makimura, Y. (2001). Layered lithium insertion material of $LiCo_{1/3}Ni_{1/3}Mn_{1/3}O_2$ for lithium-ion batteries. Chem. Lett. 642–643.

35. Sun, Y.K., Chen, Z., Noh, H.J., Lee, D.J., Jung, H.G., Ren, Y., Wang, S., Yoon, C.S., Myung, S.T., and Amine, K. (2012). Nanostructured high-energy cathode materials for advanced lithium batteries. Nat. Mater. *11*, 942–947.

36. Song, J., Li, B., Chen, Y., Zuo, Y., Ning, F., Shang, H., Feng, G., Liu, N., Shen, C., Ai, X., et al. (2020). A high-performance Li-Mn-O Li-rich cathode material with rhombohedral symmetry via intralayer Li/Mn disordering. Adv. Mater. *32*, e2000190.

37. Rossouw, M.H., Liles, D.C., and Thackeray, M.M. (1993). Synthesis and structural characterization of a novel layered lithium manganese oxide, $Li_{0.36}Mn_{0.91}O_2$, and its lithiated derivative, $Li_{1.09}Mn_{0.91}O_2$. J. Solid State Chem. *104*, 464–466.

38. Thackeray, M.M., Johnson, C.S., Vaughey, J.T., Li, N., and Hackney, S.A. (2005). Advances in manganese-oxide 'composite' electrodes for lithium-ion batteries. J. Mater. Chem. *15*, 2257.

39. Yu, H., So, Y.G., Kuwabara, A., Tochigi, E., Shibata, N., Kudo, T., Zhou, H., and Ikuhara, Y. (2016). Crystalline grain interior configuration affects lithium migration kinetics in Li-rich layered oxide. Nano Lett. *16*, 2907–2915.

40. Zuo, Y., Li, B., Jiang, N., Chu, W., Zhang, H., Zou, R., and Xia, D. (2018). A high-capacity O_2-type Li-rich cathode material with a single-layer Li_2MnO_3 superstructure. Adv. Mater. *30*, e1707255.

41. Wu, T., Liu, X., Zhang, X., Lu, Y., Wang, B., Deng, Q., Yang, Y., Wang, E., Lyu, Z., Li, Y., et al. (2020). Full concentration gradient-tailored Li-rich layered oxides for high-energy lithium-ion batteries. Adv. Mater. e2001358.

42. Grey, C.P., and Tarascon, J.M. (2016). Sustainability and in situ monitoring in battery development. Nat. Mater. *16*, 45–56.

43. Mineral commodity summaries 2019: U.S. Geological Survey. https://www.usgs.gov/centers/nmic/mineral-commodity-summaries.

44. Ceder, G., and Mishra, S.K. (1999). The stability of orthorhombic and monoclinic-layered $LiMnO_2$. Electrochem. Solid State Lett. *2*, 11.

45. Jahn, H.A., and Teller, E. (1937). Stability of polyatomic molecules in degenerate electronic states. Proc. R. Soc. A. *161*, 220–235.

46. Radin, M.D., and Van der Ven, A. (2018). Simulating charge, spin, and orbital ordering: application to Jahn–Teller distortions in layered transition-metal oxides. Chem. Mater. *30*, 607–618.

47. Rougier, A., and Delmas, C. (1995). Non-cooperative Jahn–Teller effect in $LiNiO_2$: an EXAFS study. Solid State Comm. *94*, 123–127.

48. Ohzuku, T., Kate, J., Sawai, K., and Hirai, T. (1991). Electrochemistry of manganese dioxide in lithium nonaqueous cells: IV. Jahn–Teller deformation of MnO_6-octahedron in Li_xMnO_2. J. Electrochem. Soc. *138*, 2556.

49. Prasad, R., Benedek, R., Kropf, A.J., Johnson, C.S., Robertson, A.D., Bruce, P.G., et al. (2003). Divalent-dopant criterion for the suppression of Jahn–Teller distortion in Mn oxides: first-principles calculations and X-ray absorption spectroscopy measurements for Co in $LiMnO_2$. Phys. Rev. B *68*, 012101, https://doi.org/10.1103/PhysRevB.68.012101.

50. Huang, Z.-F., Du, F., Wang, C.-Z., Wang, D.-P., and Chen, G. (2007). Low-spin Mn^{3+} ion in rhombohedral $LiMnO_2$ predicted by first-principles calculations. Phys. Rev. B *75*, 054411.

51. Matsumoto, N., Sunatsuki, Y., Miyasaka, H., Hashimoto, Y., Luneau, D., and Tuchagues, J.-P. (1999). [{Mn(salen)CN}$_n$]: the first one-dimensional chain with alternating high-spin and low-spin Mn^{III} centers exhibits metamagnetism. Angew. Chem. Int. Ed. *38*, 171–173.

52. Whittingham, M.S. (2004). Lithium batteries and cathode materials. Chem. Rev. *104*, 4271–4301.

53. Thackeray, M.M., Johnson, P.J., De Picciotto, L.A., Bruce, P.G., and Goodenough, J.B. (1984). Electrochemical extraction of lithium from $LiMn_2O_4$. Mat. Res. Bull. *19*, 179–187.

54. David, W.I.F., Thackeray, M.M., De Picciotto, L.A., and Goodenough, J.B. (1986). Structure refinement of the spinel-related phases $Li_2Mn_2O_4$ and $Li_{0.2}Mn_2O_4$. J. Solid State Chem. *67*, 316–323.

55. Yaghoobnejad Asl, H., and Manthiram, A. (2020). Reining in dissolved transition-metal ions. Science *369*, 140–141.

56. Zhao, J., Liang, Y., Zhang, X., Zhang, Z., Wang, E., He, S., Wang, B., Han, Z., Lu, J., Amine, K., et al. (2020). In situ construction of uniform and robust cathode-electrolyte interphase for Li-rich layered oxides. Adv. Funct. Mater. 2009192.

57. Xia, Y., Zhou, Y., and Yoshio, M. (1997). Capacity fading on cycling of 4 V Li/$LiMn_2O_4$ cells. J. Electrochem. Soc. *144*, 2593.

58. Zhan, C., Wu, T., Lu, J., and Amine, K. (2018). Dissolution, migration, and deposition of transition metal ions in Li-ion batteries exemplified by Mn-based cathodes – a critical review. Energy Environ. Sci. *11*, 243–257.

59. Liang, G., Peterson, V.K., See, K.W., Guo, Z., and Pang, W.K. (2020). Developing high-voltage spinel $LiNi_{0.5}Mn_{1.5}O_4$ cathodes for high-energy-density lithium-ion batteries: current achievements and future prospects. J. Mater. Chem. A *8*, 15373–15398.

60. Kim, J.-H., Myung, S.T., Yoon, C.S., Kang, S.G., and Sun, Y.K. (2004). Comparative study of $LiNi_{0.5}Mn_{1.5}O_{4-\delta}$ and $LiNi_{0.5}Mn_{1.5}O_4$. Chem. Mater. *16*, 906–914.

61. Liang, G., Wu, Z., Didier, C., Zhang, W., Cuan, J., Li, B., Ko, K.Y., Hung, P.Y., Lu, C.Z., Chen, Y., et al. (2020). A long cycle-life high-voltage spinel lithium-ion battery electrode achieved by site-selective doping. Angew. Chem. Int. Ed. *59*, 10594–10602.

62. Zuo, C., Hu, Z., Qi, R., Liu, J., Li, Z., Lu, J., Dong, C., Yang, K., Huang, W., Chen, C., et al. (2020). Double the capacity of manganese spinel for lithium-ion storage by suppression of cooperative Jahn–Teller distortion. Adv. Energy Mater. *10*, 2000363.

63. Zhang, W., Seo, D.-H., Chen, T., Wu, L., Topsakal, M., Zhu, Y., Lu, D., Ceder, G., and Wang, F. (2020). Kinetic pathways of ionic transport in fast-charging lithium titanate. Science *367*, 1030–1034.

64. Zhang, X., and Yu, H. (2020). Crystalline domain battery materials. Acc. Chem. Res. *53*, 368–379.

65. Zhao, S., Yan, K., Zhang, J., Sun, B., and Wang, G. (2020). Reviving reaction mechanism of layered lithium-rich cathode materials for high-energy lithium-ion battery. Angew. Chem. Int. Ed. *59*, 2–15.

66. Yu, H., So, Y.G., Ren, Y., Wu, T., Guo, G., Xiao, R., Lu, J., Li, H., Yang, Y., Zhou, H., et al. (2018). Temperature-sensitive structure evolution of lithium-manganese-rich layered oxides for lithium-ion batteries. J. Am. Chem. Soc. *140*, 15279–15289.

67. Wang, E., Zhao, Y., Xiao, D., Zhang, X., Wu, T., Wang, B., Zubair, M., Li, Y., Sun, X., and Yu, H. (2020). Composite nanostructure construction on the grain surface of Li-rich layered oxides. Adv. Mater. e1906070.

68. Seo, D.H., Lee, J., Urban, A., Malik, R., Kang, S., and Ceder, G. (2016). The structural and chemical origin of the oxygen redox activity in layered and cation-disordered Li-excess cathode materials. Nat. Chem. *8*, 692–697.

69. Hu, E., Yu, X., Lin, R., Bi, X., Lu, J., Bak, S., Nam, K.-W., Xin, H.L., Jaye, C., Fischer, D.A., et al. (2018). Evolution of redox couples in Li- and Mn-rich cathode materials and mitigation of voltage fade by reducing oxygen release. Nat. Energy *3*, 690–698.

70. Liu, S., Liu, Z., Shen, X., Wang, X., Liao, S.C., Yu, R., Wang, Z., Hu, Z., Chen, C.T., Yu, X., et al. (2019). Li-Ti cation mixing enhanced structural and performance stability of Li-rich layered oxide. Adv. Energy Mater. *9*, 1901530.

71. Pang, W.K., Lin, H.-F., Peterson, V.K., Lu, C.-Z., Liu, C.-E., Liao, S.-C., and Chen, J.-M. (2017). Effects of fluorine and chromium doping on the performance of lithium-rich $Li_{1+x}MO_2$ (M = Ni, Mn, Co) positive electrodes. Chem. Mater. *29*, 10299–10311.

72. Kang, K., Meng, Y.S., Julien, B., Grey, C.P., and Ceder, G. (2006). Electrodes with high power and high capacity for rechargeable lithium batteries. Science *311*, 977–980.

73. Shi, J.L., Zhang, J.N., He, M., Zhang, X.D., Yin, Y.X., Li, H., Guo, Y.G., Gu, L., and Wan, L.J. (2016). Mitigating voltage decay of Li-rich cathode material via increasing Ni content for lithium-ion batteries. ACS Appl. Mater. Interfaces *8*, 20138–20146.

74. Qing, R.-P., Shi, J.-L., Xiao, D.-D., Zhang, X.-D., Yin, Y.-X., Zhai, Y.-B., Gu, L., and Guo, Y.-G. (2016). Enhancing the kinetics of Li-rich cathode materials through the pinning effects of gradient surface Na^{+} doping. Adv. Energy Mater. *6*, 1501914.

75. Li, Q., Li, G., Fu, C., Luo, D., Fan, J., and Li, L. (2014). K^{+}-doped $Li_{1.2}Mn_{0.54}Co_{0.13}Ni_{0.13}O_2$: a novel cathode material with an enhanced cycling stability for lithium-ion batteries. ACS Appl. Mater. Interfaces *6*, 10330–10341.

76. An, J., Shi, L., Chen, G., Li, M., Liu, H., Yuan, S., Chen, S., and Zhang, D. (2017). Insights into the stable layered structure of a Li-rich cathode material for lithium-ion batteries. J. Mater. Chem. A *5*, 19738–19744.

77. Zhang, H.Z., Qiao, Q.Q., Li, G.R., and Gao, X.P. (2014). PO_4^{3-} polyanion-doping for stabilizing Li-rich layered oxides as cathode materials for advanced lithium-ion batteries. J. Mater. Chem. A *2*, 7454–7460.

78. Thackeray, M.M., Kang, S.-H., Johnson, C.S., Vaughey, J.T., Benedek, R., and Hackney, S.A. (2007). Li_2MnO_3-stabilized $LiMO_2$ (M = Mn, Ni, Co) electrodes for lithium-ion batteries. J. Mater. Chem. *17*, 3112.

79. Baur, W.H. (1973). The geometry of polyhedral distortions. Predictive relationships for the phosphate group. Acta Cryst. *B30*, 1195–1215.

80. Wang, Y., Wang, L., Guo, X., Wu, T., Yang, Y., Wang, B., Wang, E., and Yu, H. (2020). Thermal stability enhancement through structure modification on the microsized crystalline grain surface of lithium-rich layered oxides. ACS Appl. Mater. Interfaces *12*, 8306–8315.

81. Uyama, T., Mukai, K., and Yamada, I. (2019). Synthesis of rhombohedral $LiCo_{0.64}Mn_{0.36}O_2$ using a high-pressure method. Inorg. Chem. *58*, 6684–6695.

82. Wang, Y., Wang, E., Zhang, X., and Yu, H. (2021). High-voltage "single-crystal" cathode materials for lithium-ion batteries. Energy Fuels *35*, 1918–1932.

83. Cao, X., Li, H., Qiao, Y., Jia, M., Li, X., Cabana, J., and Zhou, H. (2020). Stabilizing anionic redox chemistry in a Mn-based layered oxide cathode constructed by Li-deficient pristine state. Adv. Mater. e2004280.

84. Shang, H., Zuo, Y., Shen, F., Song, J., Ning, F., Zhang, K., He, L., and Xia, D. (2020). O_2-type $Li_{0.78}[Li_{0.24}Mn_{0.76}]O_2$ nanowires for high-performance lithium-ion battery cathode. Nano Lett. *20*, 5779–5785.

85. Huang, Z.-F., Meng, X., Wang, C.-Z., Sun, Y., and Chen, G. (2006). First-principles calculations on the Jahn–Teller distortion in layered $LiMnO_2$. J. Power Sources *158*, 1394–1400.

86. Liu, X., Wang, X., Iyo, A., Yu, H., Li, D., and Zhou, H. (2014). High stable post-spinel $NaMn_2O_4$ cathode of sodium ion battery. J. Mater. Chem. A *2*, 14822–14826.

87. Darul, J., Lathe, C., and Piszora, P. (2014). Hooked on switch: strain-managed cooperative Jahn–Teller effect in $Li_{0.95}Mn_{2.05}O_4$ spinel. RSC Adv. *4*, 65205–65212.

88. Shang, Y., Li, X., Song, J., Huang, S., Yang, Z., Xu, Z.J., and Yang, H.Y. (2020). Unconventional Mn vacancies in Mn–Fe Prussian blue analogs: suppressing Jahn–Teller distortion for ultrastable sodium storage. Chem *6*, 1804–1818.

89. Hohenberg, P., and Kohn, W. (1964). Inhomogeneous electron gas. Phys. Rev. *136*, B864–B871.

90. Blochl, P.E. (1994). Projector augmented-wave method. Phys. Rev. B *50*, 17953–17979.